Research Article

For reprint orders, please contact: reprints@futuremedicine.com

Epigenomics

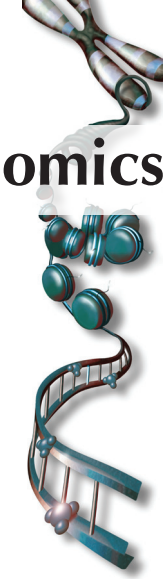

Epigenetic changes and functional study of *HOXA11* in human gastric cancer

Aim: To examine epigenetic changes and the function of *HOXA11* in human gastric cancer (GC). **Materials & methods:** Seven GC cell lines, five cases of normal gastric mucosa and 112 cases primary GC samples were used in this study. **Results:** Expression of *HOXA11* and lack of promoter region methylation were found in NCI-N87, MKN45, BGC823 and HGC27 cells. Loss of expression and complete methylation were found in AGS gastric cancer cells. Reduced expression and partial methylation were found in MGC803 and SGC7901 cells. Restoration of *HOXA11* expression was induced by 5-aza-2′-deoxycytidine. *HOXA11* was methylated in 81.25% (91/112) of primary GCs. The presence of methylation was associated with male gender, tumor size, tumor differentiation and lymph node metastasis (all $p < 0.05$). Restoration of *HOXA11* expression reduced cell proliferation, invasion, migration and induced apoptosis and G2/M phase arrest. HOXA11 was found to inhibit Wnt signaling by upregulating NKD1 expression. **Conclusion:** Epigenetic silencing of *HOXA11* promotes GC proliferation, migration and invasion through activation of Wnt signaling.

Keywords: 5-aza-2′-deoxycytidine • DNA methylation • epigenetics • gastric carcinoma • *HOXA11* • invasion • migration • NKD1 • tumor suppressor • Wnt signaling pathway

Yingying Cui[‡,1], Dan Gao[‡,1,2], Enqiang Linghu[1], Qimin Zhan[3], Runsheng Chen[4], Malcolm V Brock[5], James G Herman[6] & Mingzhou Guo*[,1]

[1]Department of Gastroenterology & Hepatology, Chinese PLA General Hospital, Beijing, China
[2]Medical College of NanKai University, Tianjin, China
[3]State Key Laboratory of Molecular Oncology, Cancer Institute & Hospital, Chinese Academy of Medical Sciences & Peking Union Medical College, Beijing, China
[4]Laboratory of Noncoding RNA, Institute of Biophysics, Chinese Academy of Sciences, Beijing, China
[5]Sidney Kimmel Comprehensive Cancer Center, Johns Hopkins University, Baltimore, MD 21231, USA
[6]The Hillman Cancer Center, University of Pittsburgh Cancer Institute, Pittsburgh, PA 15213, USA
*Author for correspondence:
Tel.: +86 10 66937651
Fax: +86 10 68180325
mzguo@hotmail.com
[‡]Authors contributed equally

Gastric cancer (GC) is the fourth most common malignancy and ranks the second leading cause of cancer-related death in the world [1,2]. Salt, nitrite, alcohol, smoking and *Helicobacter pylori* infection were regarded as important risk factors [3]. Even though aberrant genetic changes play critical roles, they are not enough to explain the mechanism of gastric carcinogenesis [4,5]. Epigenetics is becoming one of the important fields of cancer research. Increasing evidence suggests that epigenetics is involved in gastric carcinogenesis [6,7]. *HOX* genes are evolutionarily conserved genes encoding transcription factors that regulate mammalian embryonic development [8,9]. *HOXA11* plays an important role in regulating cell differentiation and proliferation [10,11]. Promoter region hypermethylation of *HOXA11* was found in different human cancers [12–15]. The epigenetic changes and the function of *HOXA11* in human gastric cancer remain unclear. In this study, we analyzed the epigenetic regulation and the mechanism of *HOXA11* in the development of human gastric cancer.

Materials & methods

Primary GC samples

One hundred and twelve cases of GC samples were collected from the Chinese PLA General Hospital. The median age of cancer patients was 58.5 years (17–85 years). Tumor stage was classified according to TNM staging (NCCN2012), including stage IIA (n = 4), stage IIB (n = 12), stage IIIA (n = 9), stage IIIB (n = 48), stage IIIC (n = 15), stage IV (n = 24). Five cases of normal gastric mucosa were collected from noncancerous patients. All samples were collected according to the approved guidelines of the Chinese PLA General Hospital's institutional review board and kept at -80°C.

Future Medicine part of fsg

Cell culture & 5-aza-2′-deoxycytidine treatment

Seven GC cell lines were included in this study (AGS, NCI-N87, SGC7901, MGC803, BGC823, HGC27 and MKN45). The GC cell lines were established from primary human gastric adenocarcinoma cells previously and maintained in 90% RPMI 1640 (Invitrogen, CA, USA), supplemented with 10% fetal bovine serum and antibiotics [16]. GC cells were split to a low density (30% confluence) 12 h before treatment, then treated with 5-aza-2′-deoxycytidine (5-aza; Sigma, MO, USA) at a concentration of 2 μM in the growth medium, which was exchanged every 24 h for total 96 h treatment. At the end of the treatment course, RNA was isolated as described below.

RNA isolation & semiquantitative RT-PCR

Total RNA was isolated by Trizol reagent (Invitrogen, Carlsbad, USA). RNA quality and quantity were evaluated by 1% Agarose gel electrophoresis and spectrophotometric analysis. Semiquantitative reverse transcription-PCR (RT-PCR) was performed as described previously [17]. RT-PCR primers were as follows: (F) 5′-GCAGCAGAGGAGAAAGAGCG-3′ and (R) 5′- GTGGATTTGCTGAGTAGTACTG-3′.

DNA extraction, methylation-specific PCR & bisulfite sequencing

Genomic DNA from GC cell lines and GC tissue samples was prepared by proteinase-K method. Methylation-specific PCR (MSP) and bisulfite sequencing (BSSQ) were performed as described previously [18,19]. To obtain optimal conversion of cytosine to uracil by bisulfite treating, 1 μg genomic DNA was used, because increasing the amount of input DNA carried the risk of incomplete conversion and led to false-positive results [20]. Sodium bisulfite treated-DNA should be treated as RNA and stored at-20°C to prevent further degradation. It is important to avoid repeated freezing and thawing. Bisulfite sequencing was used to validate MSP result and provide complete CpG methylation information on all CpG-sites within the PCR product.

Each MSP reaction incorporated approximately 100 ng of bisulfite-treated DNA, 25 pmoles of each primer, 100 pmoles dNTPs, 2.5 ul 10× PCR buffer and 1 unit of JumpStart Red Taq Polymerase (Sigma) in a final reaction volume of 25 μl. Cycle conditions were: 95° C × 5 min; 35 cycles × (95°C × 30 s, 60°C × 30 s, 72°C × 30 s); 72° C × 5 min. MSP products were analyzed using 2% agarose gel electrophoresis. To interpret the MSP results properly, positive, negative and H2O controls were included. MSP primers and BSSQ primers were designed around the transcriptional start site. To accomplish optimal discriminative power between methylated and unmethylated DNA, the primers should have a substantial number of non-CpG cytosines in the original template and contain one to three CpG dinucleotides in the 3′region of the primers [20]. The sequences of *HOXA11* MSP primers were as follows: (UF) 5′-TGTGTGTGAAGTGATTTTTAGAGAGTAT-3′, (UR)5′-AACAATCTCTATACACAAACTCCTCCA-3′; (MF) 5′-TGCGCGAAGTGATTTTTAGAGAGTAC-3′,(MR)5′-CAATCTCTATACACGAACTCCTCCG-3′. Primer sequences of BSSQ were: (F)5′-GTTTYGGGTTTAGATTTTTTTAGT-3′, (R)5′-TAACCRAACTCTTAACCAACAC-3′. The unmethylated (U) primer will only amplify sodium bisulfite converted DNA in unmethylated condition, while the methylated (M) primer is specific for sodium bisulfite converted methylated DNA. Sample was regarded as unmethylation when PCR product was amplified only in unmethylation reaction and sample was regarded as methylation when amplified only in methylation reaction. Sample amplified in both unmethylation and methylation reaction was regarded as partial methylation. Since clinical tissue samples should be considered heterogeneous, both unmethylation and methylation amplicons can be expected.

Immunohistochemistry

Immunohistochemistry (IHC) staining was performed in 45 cases of available matched cancer and adjacent noncancerous tissue samples. The procedure was performed as described previously [17]. Immunohistochemistry (IHC) was performed on 4 μm thick serial sections derived from formaldehyde-fixed paraffin blocks of colorectal cancer and paired adjacent tissue. After deparaffinization and rehydration, endogenous peroxidase activity was blocked for 30 min in methanol containing 0.3% hydrogen peroxide. After antigen retrieval, a cooling-off period of 20 min preceded the incubation with the primary antibody. Anti-HOXA11 Mouse Monoclonal (8B8) was diluted to 1/200 (LifeSpan BioScience, MD, USA), anti-p-β-catenin was diluted to 1/100 (Bioword, Shanghai, China). The staining intensity and extent of the staining area were graded according to the German semiquantitative scoring system as described before [17,21,22]. Staining intensity of the nucleus, cytoplasm and/or membrane was characterized as follows: no staining = 0, weak staining = 1, moderate staining = 2, strong staining = 3; the extent of staining was defined as: 0% = 0, 1–24% = 1, 25–49% = 2, 50–74% = 3, 75–100% = 4. The final immune-reactive score (0–12) was determined by multiplying intensity score by the extent of staining score.

HOXA11 expression plasmid construction

The full length complementary DNA (cDNA) of *HOXA11* was obtained by RT-PCR. The primers were as follows: *HOXA11*-EGFPN1-F: 5′- CGGAATTCATGGATTTTGATGAGCGTGGTCCCT-3′; *HOXA11*-EGFPN1-R: 5′- CGGGATCCCGGAGGAGTGGATTTGCTGAGTAG-3′. The products were subcloned into pcDNA™ 3.1 expression vector.

shRNA knock down assay

ShRNA sequences of *HOXA11* are as follows: (F) 5′-GATCCGCCCAATGACATACTCCTACTTTCAAGAGAAGTAGGAGTATGT-CATTGGGCTTTTTTGGAAA-3′; (R) 5′-AGCTTTTCCAAAAAA GCCCAATGACATACTCCTAC-TAAGTTCTCTAGTAGGAGTATGT-CATTGGGCG-3′. The scramble control non-targeting short-hairpin RNA sequence was 5′-TTCTCCGAACGTGTCACGT-3′ (Ambion Inc., TX, USA).

Transfection

AGS cells were transfected with pCDNA3.1-*HOXA11* or the empty vector using FuGENE 6 (Roche Applied Science, IN, USA) according to manufacturer's instructions. BGC823 cells were transfected with *HOXA11*-shRNA or scramble control using FuGENE 6 (Roche Applied Science).

Colony formation & cell viability detection

Cells were seeded at a density of 2000 cells/well in 6-well plates to grow for 2 weeks. Then cells were fixed with 75% ethanol for 30 min, stained with 0.2% crystal violet (Beyotime, Nanjing, China) for 20 min and then the number of clones was counted. Cells were plated in 96-well plates at a density of 2×10^3 cells/well, and cell viability was measured at 24, 48 and 72 h using the MTT assay (KeyGEN Biotech, Nanjing, China) according to the manufacturer's instruction. Absorbance was measured on a microplate reader (Thermo Multiskan MK3, MA, USA) at a wavelength of 490 nm.

Transwell assay for migration

The effect of *HOXA11* on cell migration was detected by using Transwell Assay System (Corning, High Wyombe, UK). Cells were harvested and suspended in the serum-free medium and then placed into the upper well at a concentration of 2×10^5 cells/200 µl. The complete medium with 20% fetal bovine serum was placed into the lower well (600 µl). The chamber was incubated for 24 h. The cells still on the upper surface were scraped gently and washed out with PBS for three-times. The cells migrated to the lower surface of the membrane were stained with crystal violet and counted in three independent high-power fields (×200).

Transwell assay for invasion

A total of 1×10^5 cells were suspended in 200 µl of serum-free medium and loaded onto the upper compartment of an invasion chamber containing a polycarbonate membrane with an 8 µm pore size which was coated with a layer of extracellular matrix (ECM; Matrigel™, BD, NJ, USA). After 24 h of incubation, the invasive cells migrating through the ECM layer to the complete medium in the lower compartment were stained with crystal violet and the number of invasive cells was counted in three independent high-power fields (×200).

Flow cytometry analysis

Cell phase distribution was examined as described previously [23]. For apoptosis analysis, Annexin V-FITC/PI Apoptosis Detection Kit (KeyGEN Biotech) was conducted according to manufacturer's instructions.

Gene expression array analysis

RNA from *HOXA11* unexpressed and re-expressed AGS cells was purified using the RNeasy Mini Kit (QIAGEN, Shanghai, China) and the expression was analyzed by expression array (Agilent Human 4 × 44 k, Bio Corporation, Beijing, China).

Dual-Luciferase reporter assay

AGS cells were seeded at 2×10^4/well in 96-well plates and incubated for 24 h. The method was described previously [17]. To examine transcriptional activity driven by TCF/LEF, AGS cells were transfected with 20 ng/well Topflash reporter vector (TCF/LEF–responsive reporter, containing 4× TCF-binding sites); 2 ng/well pRL-TK and pCI-neo-β-catenin expressing vector (20 ng/well) were used to activate the reporter gene. As a negative control, another group of AGS cells were transfected with 20 ng/well Fopflash reporter vector (containing mutant TCF/LEF binding sites), 2 ng/well pRL-TK control vector and β-catenin expressing vector (20 ng/well). To detect the effect of *HOXA11* on β-catenin/TCF luciferase reporter activity, pEGFP-*HOXA11* and wild-type or mutant β-catenin were cotransfected into AGS cell. Forty-eight hours after transfection, relative luciferase activities were measured with the Dual Luciferase Reporter Assay System (Promega, Shanghai, China) according to the manufacturer's protocol. Each experiment was repeated for three-times. Statistical analysis was carried out by Student's t-test, $p < 0.05$ was considered as statistically significant difference.

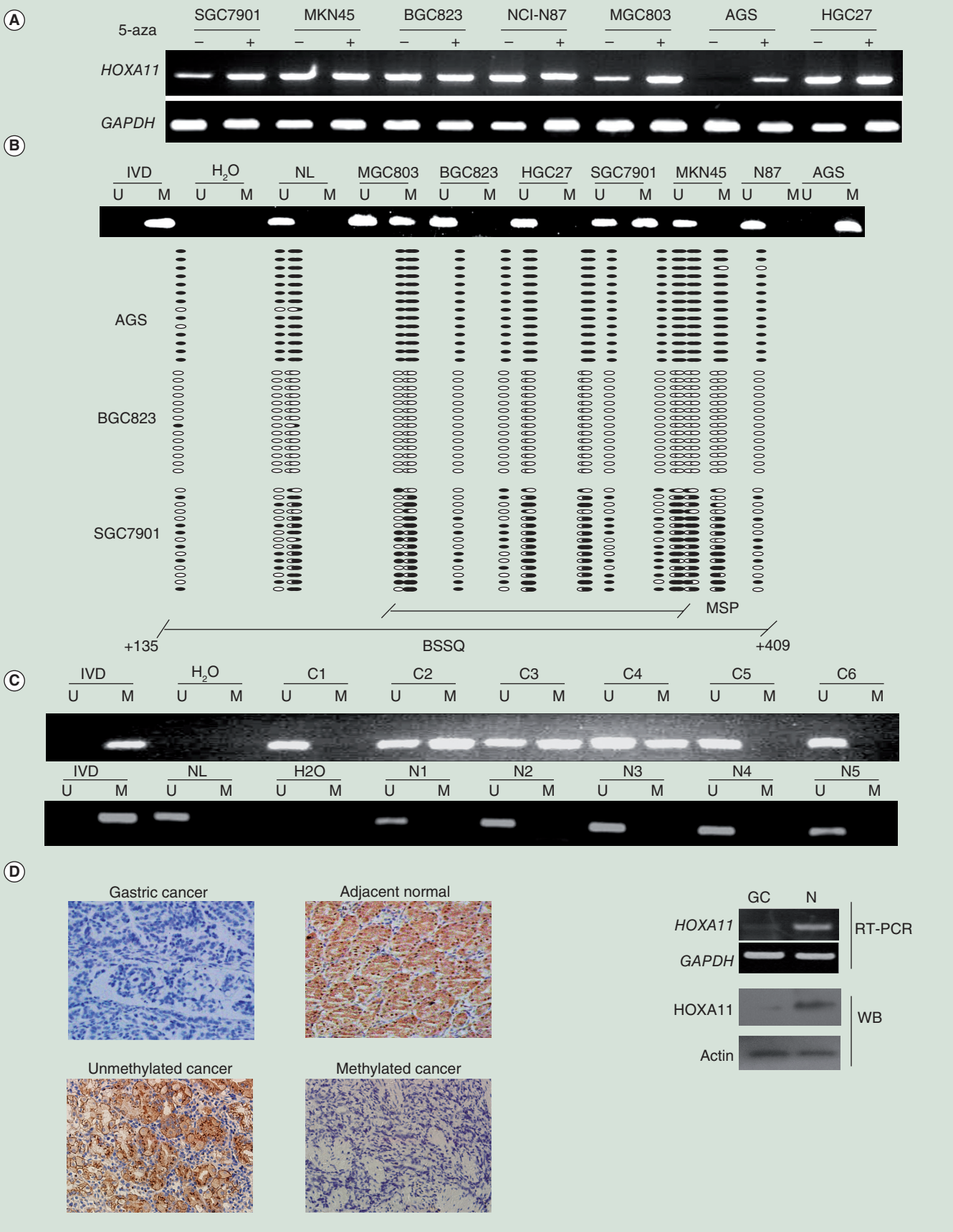
A
5-aza
SGC7901
MKN45
BGC823
NCI-N87
MGC803
AGS
HGC27
HOXA11
GAPDH
B
IVD
H2O
NL
MGC803
BGC823
HGC27
SGC7901
MKN45
N87
AGS
U M
AGS
BGC823
SGC7901
MSP
+135
BSSQ
+409
C
IVD
H2O
C1
C2
C3
C4
C5
C6
IVD
NL
H2O
N1
N2
N3
N4
N5
D
Gastric cancer
Adjacent normal
Unmethylated cancer
Methylated cancer
GC
N
HOXA11
GAPDH
RT-PCR
HOXA11
Actin
WB

Figure 1. *HOXA11* expression was regulated by promoter region methylation in gastric cancer (see facing page).
(A) The expression of *HOXA11* was detected by semiquantitative RT-PCR before and after 5-aza-2′-deoxycytidine (5-AZA) treatment in gastric cancer cell lines. GAPDH: internal control. (+): 5-AZA treatment, (-): no 5-AZA treatment; AGS, NCI-N87, SGC7901, MGC803, BGC823, HGC27 and MKN45 are gastric cancer cell lines. **(B)** Upper: *HOXA11* methylation status in gastric cancer cell lines. Lower: Bisulfite sequencing of *HOXA11* promoter region (+409 bp to +135 bp) in AGS, BGC823 and SGC7901 cell lines. MSP: MSP amplification region, spanning 274 bp. Filled circle: methylated CpG site; open circle: unmethylated CpG site. **(C)** Upper: Representative MSP results of *HOXA11* in human gastric cancer. Lower: *HOXA11* MSP results in. normal gastric mucosa. **(D)** Left: IHC results of *HOXA11* expression in gastric cancer and adjacent tissue samples (200×, upper), and the expression of *HOXA11* in promoter region unmethylated and hypermethylated gastric cancer samples (200×, lower). Right: RT-PCR and western blot results in gastric cancer and normal gastric mucosa.
C: Gastric cancer; IVD: *In vitro* methylated DNA served as methylation control; M: Methylated alleles; N: Normal gastric mucosa; NL: Normal peripheral lymphocytes DNA served as unmethylated control; U: Unmethylated alleles; H_2O: Water.

Western blot

Western blotting was performed as described previously [17]. Antibodies were diluted according to manufacturer's instruction. Antibodies employed were as follows: anti-HOXA11 Mouse Monoclonal (8B8) Antibody (LifeSpan BioScience, MD, USA), rabbit anti-Cylin D1 (Bioworld Tech., MN, USA), rabbit anti-c-Myc (Bioworld Tech.), rabbit anti-Survivin (Bioworld Tech.), rabbit anti-mmp2 (Bioworld Tech.), rabbit anti-mmp9 (Bioworld Tech.), rabbit anti-cyclinB1 (Bioworld Tech.), rabbit anti-β-catenin (Epitomics, CA, USA) and rabbit anti-p-β-catenin (CST, MA, USA).

Statistical analysis

SPSS 17.0 software was employed. χ^2 test and Student's t-test were used. Quantitative data were presented as the mean ± SD. A p-value of less than 0.05 was considered as statistical significance.

Results

HOXA11 expression is controlled by promoter region methylation in human GC cell lines

To examine the expression of *HOXA11*, semiquantitative RT-PCR was employed. Expression of *HOXA11* was found in NCI-N87, MKN45, BGC823 and HGC27 cells. Loss of expression was found in AGS cells and reduced expression was found in MGC803 and SGC7901cells (Figure 1A). The methylation status of the promoter region was determined by MSP. Complete methylation was found in AGS cells and partial methylation was found in MGC803 and SGC7901 cells. No promoter region methylation was detected in NCI-N87, MKN45, BGC823 and HGC27 cells (Figure 1B). Lost/reduced expression of *HOXA11* correlated with the promoter region methylation status very well. Restoration of *HOXA11* expression was induced by 5-AZA treatment in methylated cancer cells (Figure 1A). These results suggest that expression of *HOXA11* was controlled by promoter region methylation. To further validate the specificity of the MSP studies, and to determine the methylation density in the promoter region, sodium bisulfite sequencing was performed in AGS, BGC823 and SGC7901 cells. As shown in Figure 1B, sequencing results matched the MSP results well, with near complete, partial or absent DNA methylation.

HOXA11 was frequently methylated in human primary GCs & reduced expression correlates with promoter region hypermethylation

HOXA11 was found to be methylated in 81% (91/112) of primary gastric cancers, while no methylation was found in five cases of normal gastric mucosa (Figure 1C). Methylation of *HOXA11* was associated with male gender ($p < 0.05$), tumor size ($p < 0.05$), tumor differentiation ($p < 0.05$) and lymph node metastasis ($p < 0.05$), but no association was found with age and TNM stage (Table 1). To determine if there was an association of *HOXA11* expression and promoter region methylation in primary human GCs, the expression of *HOXA11* was evaluated using immunohistochemistry in 45 cases using matched GCs and adjacent tissue. HOXA11 staining was observed in both the nucleus and cytoplasm. In 45 cases of GC samples, absent or reduced expression was found in 37 cases. In 45 cases of adjacent tissue samples, absent or reduced expression was found in five cases. This suggests that the expression of *HOXA11* was significantly reduced in GC samples compared with normal tissues ($p < 0.05$, Figure 1D). However, of greatest importance was the correlation to promoter region DNA methylation. In the 37 cases of GC samples with absent or reduced levels of *HOXA11* expression, 36 cases were found to be methylated. In contrast, no methylation was found in the other eight cases of GC which express HOXA11. Thus repression of *HOXA11* was significantly associated with promoter region hypermethylation ($p < 0.05$, χ^2 test, Figure 1D).

HOXA11 suppresses cell proliferation in AGS cells

To evaluate the effect of *HOXA11* expression in gastric carcinomas, cell viability and colony formation were used with cell lines with different baseline expression of *HOXA11*. The colony formation decreased after restoration of *HOXA11* expression in AGS cells 572 ± 69 versus

Table 1 Clinicopathological features and *HOXA11* methylation status in gastric cancer.

Clinical factor	Total (n)	*HOXA11* methylation status		
		Methylated 81.25% (n = 91)	Unmethylated 18.75% (n = 21)	p-value (χ^2 test)
Age (years):				p = 0.2857
– <60	**49**	42	7	
– ≥60	**63**	49	14	
Gender:				p = 0.0490*
– Male	83	71	12	
– Female	29	20	9	
Alcohol abuse:				p = 0.0905
– Negative	33	30	3	
– Positive	79	61	18	
Smoking:				p = 0.6294
– Negative	37	31	6	
– Positive	75	60	15	
Tumor size (cm):				p = 0.0092*
– <5	37	25	12	
– ≥5	75	66	9	
Differentiation:				p = 0.0018
– Poor	61	56	5	
– High/moderate	51	35	16	
Tumor stage:				p = 0.2431
– II	16	12	4	
– III	71	61	10	
– IV	25	18	7	
Lymph node metastasis:				p = 0.0183*
– Positive	88	76	12	
– Negative	24	15	9	

*p-values are obtained from a χ^2 test, significant difference: $p < 0.05$.

116 ± 30 ($p < 0.05$, Figure 2B). This difference suggests that colony formation was suppressed by *HOXA11*. This activity was further confirmed by shRNA knockdown in *HOXA11* expressing BGC823 cells. The colony formation increased from 77 ± 8 to 281 ± 21 ($p < 0.05$, Figure 2A) after shRNA knockdown of *HOXA11*.

The cell viability was determined next using MTT. The OD value was 1.343 ± 0.126 versus 0.668 ± 0.098 ($p < 0.05$) before and after restoration of *HOXA11* expression in AGS cells. The OD value was 2.536 ± 0.342 versus 1.582 ± 0.181 ($p < 0.05$) before and after knocking down *HOXA11* in BGC823 cells (Figure 2B). These results suggest that *HOXA11* suppresses cell proliferation in GC cells.

HOXA11 induced G2/M arrest in GC cells

To further analyze the effect of *HOXA11* on gastric carcinogenesis, cell phase distribution was evaluated by flow cytometry in AGS cells before and after re-expression of *HOXA11*. As shown in Figure 2C, the distribution of cell phases in the AGS cell line with *HOXA11* unexpressed and re-expressed were: phase G0/1: 38.96± 1.17% versus 34.78 ± 3.57%; S phase: 42.02 ± 1.74% versus 27.13 ± 5.80%; G2/M phase: 19.68 ± 2.34% versus 46.08 ± 5.18%. The S phase was reduced significantly ($p < 0.05$) and the G2/M phase was increased significantly ($p < 0.05$). To further validate these findings, shRNA knockdown technique was used in *HOXA11* stably expressed BGC823 cells. The cell phase distribution, before and after knocking down *HOXA11*, was as follows: G0/1phase: 57.22 ± 0.07% versus 58.08 ± 2.32%; S phase: 19.42 ± 0.05% versus 40.53 ± 2.43%; G2/M phase: 22.98 ± 0.59% versus 1.38 ± 0.14% (Figure 2C). S phase was increased significantly ($p < 0.05$) and the G2/M ($p < 0.05$) was reduced significantly after knocking down *HOXA11*. These results suggest that *HOXA11* induces G2/M phase arrest in GC. To further understand the mechanism, the expression of G2/M phase regulators, cyclinB1 and cdc2, was examined by western blot before and after re-expression of *HOXA11* in AGS cells. The expression of cyclin B1 and cdc2 was reduced after re-expression of *HOXA11* (Figure 2C), providing an explanation for the observed cell cycle changes.

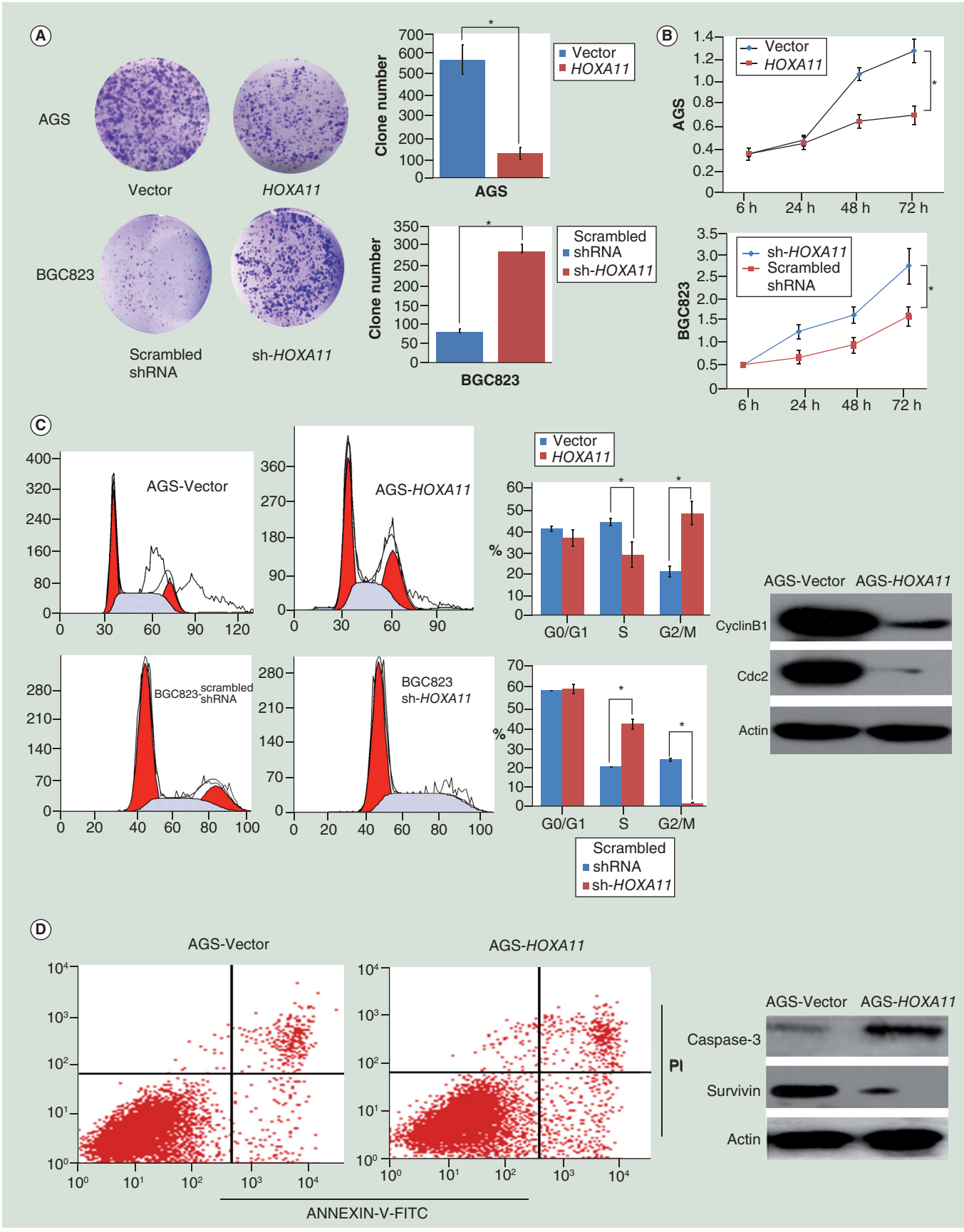
A
AGS
Vector
HOXA11
BGC823
Scrambled shRNA
sh-HOXA11
Clone number
AGS
BGC823
Vector
HOXA11
Scrambled shRNA
sh-HOXA11
B
AGS
BGC823
6 h
24 h
48 h
72 h
C
AGS-Vector
AGS-HOXA11
BGC823-scrambled shRNA
BGC823 sh-HOXA11
%
G0/G1
S
G2/M
AGS-Vector AGS-HOXA11
CyclinB1
Cdc2
Actin
D
AGS-Vector
AGS-HOXA11
ANNEXIN-V-FITC
PI
Caspase-3
Survivin
Actin

Figure 2. The effect of *HOXA11* on gastric cancer cell proliferation and apoptosis (see previous page).
(A) Upper: Representative results of colony formation in *HOXA11* unexpressed and re-expressed AGS cells. Lower: Representative results of colony formation in BGC823 cells before and after knocking down *HOXA11*. The experiment was repeated for three-times. *p < 0.05. **(B)** Upper: Growth curves in *HOXA11* unexpressed and re-expressed AGS cells analyzed by MTT assay. Lower: Growth curves before and after knocking down *HOXA11* in BGC823 cells. Time Points: 6, 24, 48 and 72 h. Each experiment were repeated for three-times. *p < 0.05. **(C)** Left: Cell phase distribution evaluated by flow cytometry in AGS and BGC823 cells. Middle: Diagrams show the cell phase distribution of AGS and BGC823 cells. Right: The expression of cyclin B1 and cdc2 detected by western blot in *HOXA11* unexpressed and expressed AGS cells. Actin: internal control. The experiment was repeated for three-times. *p < 0.05. **(D)** Left: Apoptosis results in *HOXA11* unexpressed and expressed AGS cells. Right: The expression of caspase-3, survivin detected by western blot in *HOXA11* unexpressed and expressed AGS cells. Actin: internal control.

HOXA11 induces apoptosis in human GC

To further understand the role of *HOXA11* in GC, apoptosis was analyzed by flow cytometry. The rate of apoptotic cells was 7.41 ± 0.151% versus 12.01 ± 1.73% before and after re-expression of *HOXA11* in AGS cells ($p < 0.05$, Figure 2D). Apoptosis related proteins, caspase-3 and survivin were detected by western blot. The expression of caspase-3 was increased and the expression of survivin was reduced obviously after re-expression of *HOXA11* in AGS cells (Figure 2D). These results suggest that *HOXA11* induced apoptosis in human GC.

HOXA11 inhibits GC cell migration & invasion.

Since methylation of *HOXA11* is associated with lymph node metastasis in primary GC, we explored the effect of *HOXA11* on cell migration and invasion in GC cells. The number of migrating cells decreased from 250 ± 12 to 98 ± 8 ($p < 0.05$) after re-expression of *HOXA11* in AGS cells. The number of invasive cells was also decreased from 142 ± 20 to 63 ± 10 ($p < 0.05$) after re-expression of *HOXA11* in AGS cells (Figure 3A). These effects of *HOXA11* were confirmed by knocking down *HOXA11* in BGC823 cells. As shown in Figure 3A, the number of migrating cells increased from 242 ± 34 to 827 ± 24 ($p < 0.05$) cells and the number of invasive cells increased from 170 ± 15 to 356 ± 21 ($p < 0.05$) after knocking down *HOXA11* in BGC823 cells (Figure 3B).

The mechanism by which *HOXA11* altered cell migration and invasion was further explored by determining the expression of MMP2 and MMP9, proteins associated with disruption of extracellular matrix which promote metastases. The expression of MMP2 and MMP9 were both reduced after re-expression of *HOXA11* in AGS cells (Figure 3C). These results further support the role of *HOXA11* in suppression of cell migration and invasion in GC.

Isolation and identification of cancer-related genes regulated by *HOXA11* in GC

To understand the mechanism by which *HOXA11* promotes carcinogenesis, gene expression microarray was used. The expression of 223 genes was increased and 117 genes was reduced by more than twofold in *HOXA11* re-expressed AGS cells. Among these genes, 56 were upregulated more than fourfold and 21 were down regulated more than fourfold (Figure 4A, Supplementary Table 1, see online at www.futuremedicine.com/doi/suppl/10.2217/epi.14.92). These changes in gene expression were further validated using RT-PCR. of greatest significance was the finding that *NKD1* was consistently up-regulated by re-expression of *HOXA11* in AGS cells (Figure 4B). Combined with Pathway Association Analysis (http://david.niaid.nih.gov), we identified *NKD1*, a key component of Wnt signaling for further study. Upregulation of *NKD1* was further determined by western blot. The effect of *HOXA11* up-regulating *NKD1* expression was also confirmed in the knockdown of *HOXA11* in BGC823 cells (Figure 4B).

HOXA11 inhibits Wnt/β-catenin signaling in GC cells

To confirm that *HOXA11* involves Wnt signaling in GC development, TOPflash and FOPflash reporter systems were employed in this study. As shown in Figure 4C, the activity was reduced significantly by cotransfecting *HOXA11* with wild-type or mutant β-*catenin* with TOPflash reporter in AGS cells, but no changes were found by cotransfecting *HOXA11* with β-*catenin* and FOPflash reporter.

The expression of Wnt signaling downstream genes was next examined using western blot. As shown in Figure 4D, the expression of c-Myc and cyclinD1 were both reduced and phosphorylated β-catenin (p-β-catenin) was increased after re-expression of *HOXA11* in AGS cells, even though the total β-catenin level was not significantly changed (Figure 4D). The expression of p-β-catenin was further evaluated in 45 cases of available matched primary human GC and adjacent tissue samples by IHC. p-β-catenin staining was detected in both cytoplasm and nucleus. In 45 cases of adjacent tissue samples, 36 cases were p-β-catenin positive and nine cases were negative. In 45 cases of cancer tissue samples, six cases were p-β-catenin positive and 39 cases were p-β-catenin negative (Figure 4E).

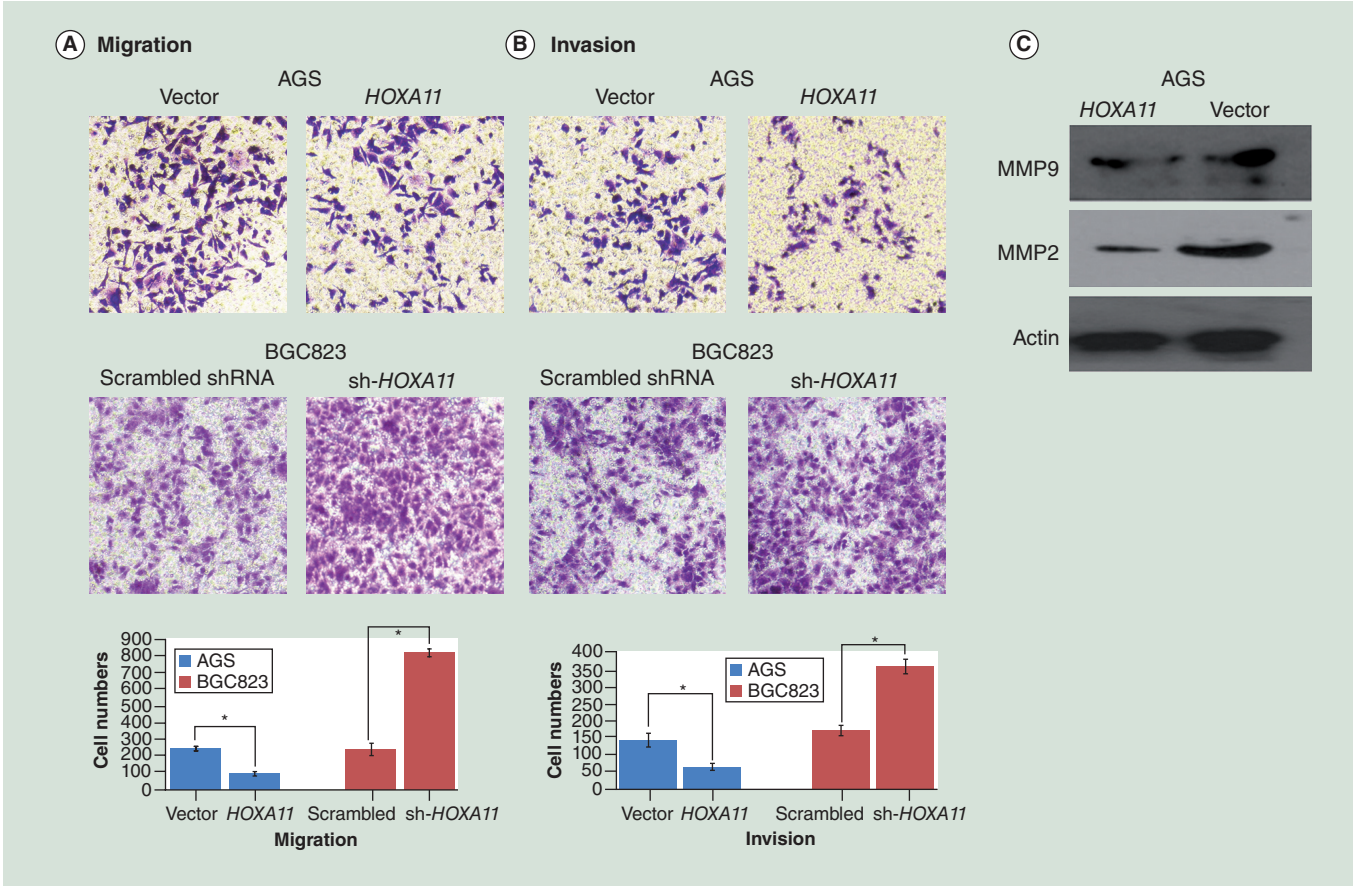

Figure 3. The effect of *HOXA11* on gastric cancer cell migration and invasion. (A) Upper: Transwell assay shows migration results in *HOXA11* unexpressed and re-expressed AGS cells. (200×) Middle: Transwell assay shows migration results before and after knocking down *HOXA11* in BGC823 cells.(200×) Lower: Bar graphs represent the numbers of migrating AGS and BGC823cells. The experiment was repeated three-times. *p < 0.05. **(B)** Upper: Transwell assay shows invasion results in *HOXA11* unexpressed and re-expressed AGS cells. (200×) Middle: Transwell assay shows invasion results before and after knocking down *HOXA11* in BGC823 cells. (200×) Lower: Bar graphs represent the numbers of invasive AGS and BGC823cells. The experiment was repeated three-times. *p < 0.05. **(C)** The expression of MMP-2 and MMP-9 detected by western blot in *HOXA11* unexpressed and re-expressed AGS cells.

HOXA11 staining and p-β-catenin staining were associated ($p < 0.05$). These results suggest that *HOXA11* function as a Wnt signaling inhibitor in human GC.

Discussion

Homeobox sequences encode the 60-amino-acid homeodomain, with a helix–turn–helix DNA binding motif [25]. In mouse and man, there are approximately 200 homeobox genes, with the 39 most homologous to the *Drosophila* homeotic genes located in four clusters (*HOXA, HOXB, HOXC* and *HOXD*) and termed *Hox* genes [26]. *HOXA11* is located in chromosome 7p15.2, a region frequently deleted in human cancers [27–29]. Larger deletions of the *HOXA* gene cluster (*HOXA1–HOXA13*) result in hand-foot-genital syndrome in combination with other malformations such as velopharyngeal insufficiency and a persistent patent ductus botalli [30]. A single *HOXA11* truncating mutation has been reported to cause a specific syndrome with skeletal defects and amegakaryocytic thrombocytopenia [31]. *HOXA11* methylation was reported in different cancers, and methylation of *HOXA11* has been proposed as an early detection marker in breast cancer [32] and a poor prognostic marker in ovarian cancer [12]. In a Phase II clinical trial, decitabine demethylation of *HOXA11* restored sensitivity to platinum in patients with platinum-resistant ovarian cancer [33]. Bai *et al.* reported that *HOXA11* expression was silenced in human GC [34]. In this study, we found that *HOXA11* was frequently methylated in human GC and expression of *HOXA11* was regulated by promoter region methylation. Methylation of *HOXA11* was associated with male gender, large tumor size, poor tumor differentiation and lymph node metastasis. *HOXA11* suppressed GC cell proliferation, invasion and migration and induced apoptosis. We found *NKD1*, a key component of Wnt signaling [35], was upregulated by *HOXA11* in GC cells, suggesting Wnt

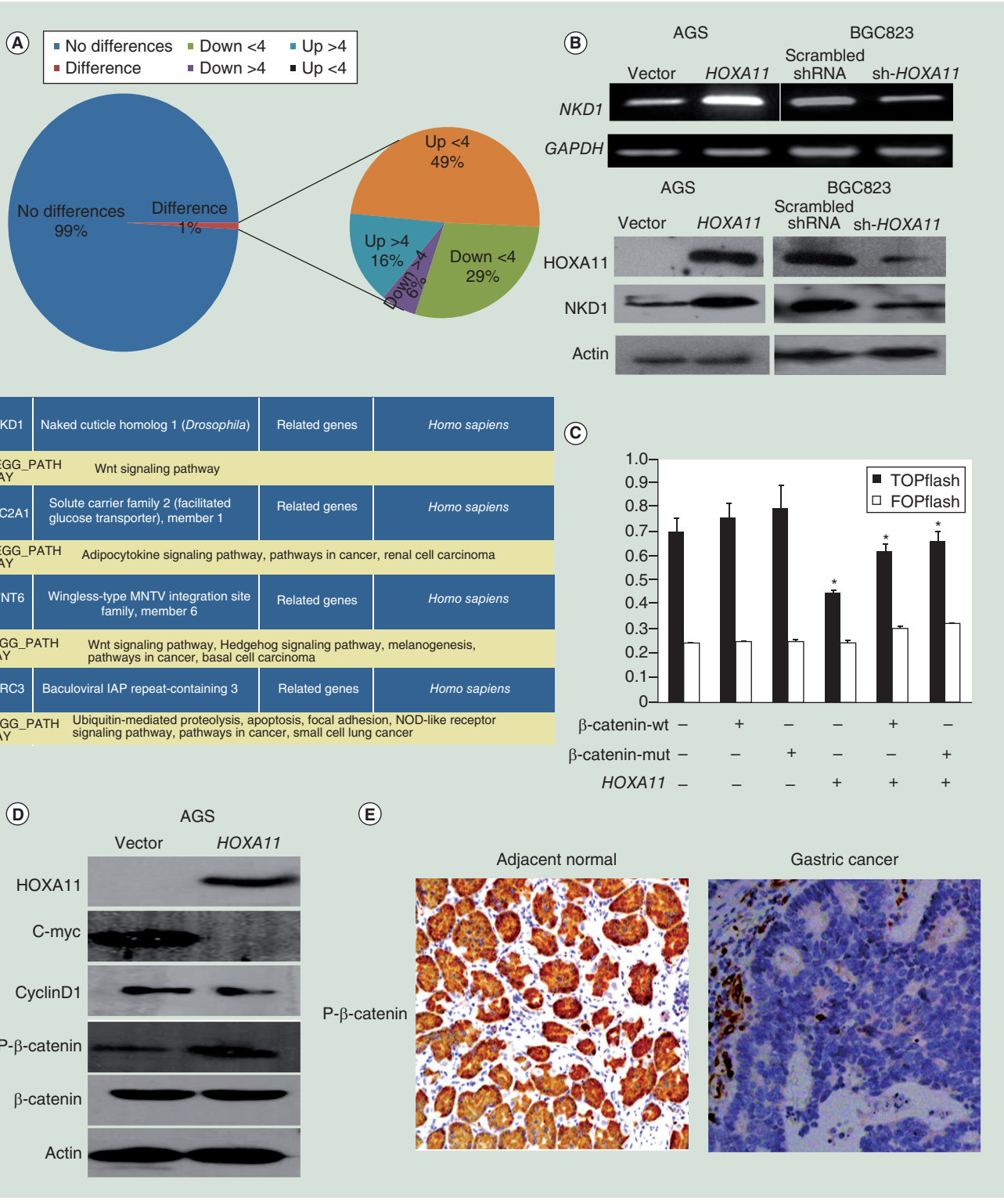

Figure 4. *HOXA11* is involved in Wnt signaling pathway in gastric cancer. (A) Gene-expression array results show differentially expressed genes in *HOXA11* unexpressed and re-expressed AGS cells. Upper: The percentage of upregulated or down regulated genes were shown in the pie chart. Lower: Representative data of pathway-related genes according to pathway-related gene analysis [24]. **(B)** The expression of *NKD1* was detected by semiquantitative RT-PCR and western blot in AGS and BGC823 cells. Actin: internal control. **(C)** Dual-Luciferase reporter assay. Luciferase activity was normalized to Renilla luciferase activity.*$p < 0.05$. **(D)** The expression of c-Myc, cyclinD1, p-β-catenin and β-catenin was detected by western blot in *HOXA11* unexpressed and re-expressed AGS cells. Actin: internal control. **(E)** IHC results of p-β-catenin expression in adjacent normal tissue and gastric cancer tissue samples.

signaling as a pathway through which *HOXA11* mediates these effects. In mice, *HOXA11* has previously been shown to interact with Wnt signaling in regulating female reproductive tract development [36]. We demonstrate that *HOXA11* was indeed inhibits Wnt signaling as demonstrated with a Luciferase reporter assay in human GC cells. The inhibiting role of *HOXA11* in Wnt signaling was further confirmed by detecting the expression of Wnt signaling downstream genes in GC cells, as well as by evaluating HOXA11 and p-β-catenin staining in human primary GC. Thus, *HOXA11* suppresses GC growth and metastasis by inhibiting Wnt signaling.

In primary tumors, quantitative methylation analysis can be considered, however, all samples retain detectable unmethylated DNA which is derived from normal tissue contamination and unmethylated tumor cells in tumors with altered DNA methylation. Thus, distinguishing the degree of methylation present is often more a measure of tumor cellularity than any functional measure of silencing. For this reason, we have not distinguished a level of methylation, but compared the presence of methylation to expression to demonstrate functional consequences of this alteration. This may alternatively have been done by real-time MSP with the establishment of cutoffs. Some genes can become aberrantly methylated during cell culture. While, our purpose is to explore the consequences of DNA methylation on silencing and downstream phenotypes in human GC. Promoter region methylation is found in 91 of the 112 primary GCs, suggesting that this is not solely a cell culture change.

In addition to 5mC (5-methylcytosine), reduction in 5hmC (5-hydroxymethylcytosine) was well reported in a number of cancers and cell lines corresponding to prostate, breast, colon, lung, brain, liver, kidney and melanoma, compared with the associated normal tissue [37–41]. But the level of 5hmC is highly variable and unreproducible [39,42]. It was undetectable in some human cancer tissues and cells [43]. 5hmC of HOXA11 was not detected in this study. The mechanism of 5hmC in human GC in *HOXA11* remains need to be elucidated.

The regulation of *HOX* gene expression has been a model to study the establishment and maintenance of heritable transcriptional states during development [44]. Polycomb (PcG) and trithorax (TrxG) proteins maintain appropriate *HOX* expression. The PRC2 complex trimethylates H3K27(me3) [45] and bind to the same histone mark that is essential for inheritable long-term repression of target genes [46]. Recruitment of PRC1 members to H3K27me3 further facilitates gene silencing. While, TrxG/MLL protein complexes catalyze the trimethylation of H3K4, which is generally associated with active transcription [47]. The regulation of HOXA11 expression by histone modification remain unclear. To better understand the mechanism of *HOXA11* expression regulating, it is necessary to analyze the promoter region histone modification status in GC.

Conclusion

HOXA11 is frequently methylated in human GC and the expression of *HOXA11* was regulated by promoter region methylation. Restoration of *HOXA11* expression suppressed cell proliferation, migration and invasion, as well as induced apoptosis and G2/M arrest. *HOXA11* suppresses GC growth by inhibiting Wnt signaling. *HOXA11* methylation is a potential GC detection and prediction marker. *HOXA11* is a Wnt signaling inhibitor that could become a therapeutic target in GC.

Future perspective

HOXA11 methylation is a potential gastric cancer detection and prediction marker, prognosis. As *HOXA11* is a Wnt signaling inhibitor, it is possible become a gastric cancer therapeutic target.

Financial & competing interests disclosure

This work was supported by grants from the National Basic Research Program (973 Program No. 2012CB934002, 2010CB912802), National Key Scientific instrument Special Programme of China (Grant No. 2011YQ03013405), National High-tech R&D Program (863 Program No. SS2012AA020314, SS2012AA020821, SS2012AA020303) and National Science Foundation of China (Grant No. 81121004, 81071953,

Executive summary

HOXA11 inhibiting Wnt signaling by upregulating NKD1 expression in human gastric cancer

- *HOXA11* is frequently methylated in human gastric cancer (GC) and the expression of *HOXA11* was regulated by promoter region methylation.
- Promoter region methylation of *HOXA11* was associated with male gender, tumor size, tumor differentiation and lymph node metastasis.
- *HOXA11* suppressed GC cell proliferation, invasion and migration, as well as induced apoptosis and G2/M phase arrest.
- *NKD1*, a key component of Wnt signaling, was up-regulated by *HOXA11*.
- *HOXA11* suppresses GC by inhibiting Wnt signaling.

81161120432). The authors have no other relevant affiliations or financial involvement with any organization or entity with a financial interest in or financial conflict with the subject matter or materials discussed in the manuscript apart from those disclosed.

No writing assistance was utilized in the production of this manuscript.

Ethical conduct

The authors state that they have obtained appropriate institutional review board approval or have followed the principles outlined in the Declaration of Helsinki for all human or animal experimental investigations. In addition, for investigations involving human subjects, informed consent has been obtained from the participants involved.

References

1 Ferlay J, Shin HR, Bray F, Forman D, Mathers C, Parkin DM. Estimates of worldwide burden of cancer in 2008: GLOBOCAN 2008. *Int. J. Cancer* 127(12), 2893–2917 (2010).

2 Jemal A, Bray F, Center MM, Ferlay J, Ward E, Forman D. Global cancer statistics. *CA Cancer J. Clin.* 61(2), 69–90 (2011).

3 Kelley JR, Duggan JM. Gastric cancer epidemiology and risk factors. *J. Clin. Epidemiol.* 56(1), 1–9 (2003).

4 Milne AN, Carneiro F, O'morain C, Offerhaus GJ. Nature meets nurture: molecular genetics of gastric cancer. *Hum. Genet.* 126(5), 615–628 (2009).

5 Panani AD. Cytogenetic and molecular aspects of gastric cancer: clinical implications. *Cancer Lett.* 266(2), 99–115 (2008).

6 Ali Z, Deng Y, Tang Y, Zheng S, Ma N, He N. Epigenetic deregulations in gastric cancer. *J. Nanosci. Nanotechnol.* 13(1), 40–51 (2013).

7 Park JH, Park J, Choi JK *et al.* Identification of DNA methylation changes associated with human gastric cancer. *BMC Med. Genomics* 4, 82 (2011).

8 Duboule D, Dolle P. The structural and functional organization of the murine *HOX* gene family resembles that of *Drosophila* homeotic genes. *EMBO J.* 8(5), 1497–1505 (1989).

9 Mcginnis W, Krumlauf R. Homeobox genes and axial patterning. *Cell* 68(2), 283–302 (1992).

10 Gross S, Krause Y, Wuelling M, Vortkamp A. *Hoxa11* and *Hoxd11* regulate chondrocyte differentiation upstream of *Runx2* and *Shox2* in mice. *PLoS ONE* 7(8), e43553 (2012).

11 Cheng W, Liu J, Yoshida H, Rosen D, Naora H. Lineage infidelity of epithelial ovarian cancers is controlled by *HOX* genes that specify regional identity in the reproductive tract. *Nat. Med.* 11(5), 531–537 (2005).

12 Fiegl H, Windbichler G, Mueller-Holzner E *et al. HOXA11* DNA methylation – a novel prognostic biomarker in ovarian cancer. *Int. J. Cancer* 123(3), 725–729 (2008).

13 Whitcomb BP, Mutch DG, Herzog TJ, Rader JS, Gibb RK, Goodfellow PJ. Frequent *HOXA11* and *THBS2* promoter methylation, and a methylator phenotype in endometrial adenocarcinoma. *Clin. Cancer Res.* 9(6), 2277–2287 (2003).

14 Hwang JA, Lee BB, Kim Y *et al. HOXA11* hypermethylation is associated with progression of non-small cell lung cancer. *Oncotarget* 4(12), 2317–2325 (2013).

15 Apostolidou S, Hadwin R, Burnell M *et al.* DNA methylation analysis in liquid-based cytology for cervical cancer screening. *Int. J. Cancer* 125(12), 2995–3002 (2009).

16 Yan W, Wu K, Herman JG *et al.* Epigenetic silencing of *DACH1* induces the invasion and metastasis of gastric cancer by activating TGF-beta signalling. *J. Cell. Mol. Med.* 18(12), 2499–2511 (2014).

17 Yan W, Wu K, Herman JG *et al.* Epigenetic regulation of *DACH1*, a novel Wnt signaling component in colorectal cancer. *Epigenetics* 8(12), 1373–1383 (2013).

18 Herman JG, Graff JR, Myohanen S, Nelkin BD, Baylin SB. Methylation-specific PCR: a novel PCR assay for methylation status of CpG islands. *Proc. Natl Acad. Sci. USA* 93(18), 9821–9826 (1996).

19 Jia Y, Yang Y, Liu S, Herman JG, Lu F, Guo M. *SOX17* antagonizes WNT/beta-catenin signaling pathway in hepatocellular carcinoma. *Epigenetics* 5(8), 743–749 (2010).

20 Derks S, Lentjes MH, Hellebrekers DM, De Bruine AP, Herman JG, Van Engeland M. Methylation-specific PCR unraveled. *Cell Oncol.* 26(5–6), 291–299 (2004).

21 Cregger M, Berger AJ, Rimm DL. Immunohistochemistry and quantitative analysis of protein expression. *Arch. Pathol. Lab. Med.* 130(7), 1026–1030 (2006).

22 Koo CL, Kok LF, Lee MY *et al.* Scoring mechanisms of p16INK4a immunohistochemistry based on either independent nucleic stain or mixed cytoplasmic with nucleic expression can significantly signal to distinguish between endocervical and endometrial adenocarcinomas in a tissue microarray study. *J. Transl. Med.* 7, 25 (2009).

23 Jia Y, Yang Y, Brock MV, Zhan Q, Herman JG, Guo M. Epigenetic regulation of *DACT2*, a key component of the Wnt signalling pathway in human lung cancer. *J. Pathol.* 230(2), 194–204 (2013).

24 Huang DW, Sherman BT, Lempicki RA. Systematic and integrative analysis of large gene lists using DAVID Bioinformatics Resources. *Nat. Protoc.* 4(1), 44–57 (2009).

25 Qian YQ, Billeter M, Otting G, Muller M, Gehring WJ, Wuthrich K. The structure of the Antennapedia homeodomain determined by NMR spectroscopy in solution: comparison with prokaryotic repressors. *Cell* 59(3), 573–580 (1989).

26 Zhao Y, Potter SS. Functional comparison of the *Hoxa 4, Hoxa 10,* and *Hoxa 11* homeoboxes. *Dev. Biol.* 244(1), 21–36 (2002).

27 Sander S, Bullinger L, Leupolt E *et al.* Genomic aberrations in mantle cell lymphoma detected by interphase fluorescence *in situ* hybridization. Incidence and clinicopathological correlations. *Haematologica* 93, 680–687 (2008).

28 Nucci MR, Harburger D, Koontz J, Dal Cin P, Sklar J. Molecular analysis of the *JAZF1–JJAZ1* gene fusion by RT-PCR and fluorescence *in situ* hybridization in endometrial stromal neoplasms. *Am. J. Surg. Pathol.* 31(1), 65–70 (2007).

29 Prokunina-Olsson L, Fu Y-P, Tang W *et al.* Refining the prostate cancer genetic association within the *JAZF1* gene on chromosome 7p15.2. *Cancer Epidemiol. Biomarkers Prev.* 19(5), 1349–1355 (2010).

30 Devriendt K, Jaeken J, Matthijs G *et al.* Haploinsufficiency of the *HOXA* gene cluster, in a patient with hand–foot–genital syndrome, velopharyngeal insufficiency, and persistent patent ductus Botalli. *Am. J. Hum. Genet.* 65(1), 249–251 (1999).

31 Fryssira H, Makrythanasis P, Kattamis A *et al.* Severe developmental delay in a patient with 7p21.1-p14.3 microdeletion spanning the *TWIST* gene and the *HOXA* gene cluster. *Mol. Syndromol.* 2(1), 45–49 (2011).

32 Tommasi S, Karm DL, Wu X, Yen Y, Pfeifer GP. Methylation of homeobox genes is a frequent and early epigenetic event in breast cancer. *Breast Cancer Res.* 11(1), R14 (2009).

33 Matei D, Fang F, Shen C *et al.* Epigenetic resensitization to platinum in ovarian cancer. *Cancer Res.* 72(9), 2197–2205 (2012).

34 Bai Y, Fang N, Gu T *et al. HOXA11* gene is hypermethylation and aberrant expression in gastric cancer. *Cancer Cell Int.* 14(1), 79 (2014).

35 Van Raay TJ, Coffey RJ, Solnica-Krezel L. Zebrafish *Naked1* and *Naked2* antagonize both canonical and non-canonical *Wnt* signaling. *Dev. Biol.* 309(2), 151–168 (2007).

36 Mericskay M, Kitajewski J, Sassoon D. *Wnt5a* is required for proper epithelial-mesenchymal interactions in the uterus. *Development* 131(9), 2061–2072 (2004).

37 Haffner MC, Chaux A, Meeker AK *et al.* Global 5-hydroxymethylcytosine content is significantly reduced in tissue stem/progenitor cell compartments and in human cancers. *Oncotarget* 2(8), 627–637 (2011).

38 Jin SG, Jiang Y, Qiu R *et al.* 5-Hydroxymethylcytosine is strongly depleted in human cancers but its levels do not correlate with *IDH1* mutations. *Cancer Res.* 71(24), 7360–7365 (2011).

39 Laird A, Thomson JP, Harrison DJ, Meehan RR. 5-hydroxymethylcytosine profiling as an indicator of cellular state. *Epigenomics* 5(6), 655–669 (2013).

40 Nestor CE, Ottaviano R, Reddington J *et al.* Tissue type is a major modifier of the 5-hydroxymethylcytosine content of human genes. *Genome Res.* 22(3), 467–477 (2012).

41 Yang H, Liu Y, Bai F *et al.* Tumor development is associated with decrease of *TET* gene expression and 5-methylcytosine hydroxylation. *Oncogene* 32(5), 663–669 (2013).

42 Ficz G, Gribben JG. Loss of 5-hydroxymethylcytosine in cancer: cause or consequence? *Genomics* 104(5), 352–357 (2014).

43 Dahl C, Gronbaek K, Guldberg P. Advances in DNA methylation: 5-hydroxymethylcytosine revisited. *Clin. Chim. Acta* 412(11–12), 831–836 (2011).

44 Soshnikova N, Duboule D. Epigenetic regulation of vertebrate *Hox* genes: a dynamic equilibrium. *Epigenetics* 4(8), 537–540 (2009).

45 Cao R, Wang L, Wang H *et al.* Role of histone H3 lysine 27 methylation in Polycomb-group silencing. *Science* 298(5595), 1039–1043 (2002).

46 Francis NJ, Follmer NE, Simon MD, Aghia G, Butler JD. Polycomb proteins remain bound to chromatin and DNA during DNA replication *in vitro*. *Cell* 137(1), 110–122 (2009).

47 Briggs SD, Bryk M, Strahl BD *et al.* Histone H3 lysine 4 methylation is mediated by Set1 and required for cell growth and rDNA silencing in *Saccharomyces cerevisiae*. *Genes Dev.* 15(24), 3286–3295 (2001).